A mathematical model to quantify dynamic forces in the powertrain of torque regulated movable bridge machineries

K. Sektani, A. Tsouvalas, A. Metrikine
Faculty of Civil Engineering and Geosciences, Delft University of Technology,
Stevinweg 1, 2628 CN Delft, the Netherlands (k.sektani@tudelft.nl)

The reassessment of existing movable bridges in The Netherlands has created the need for acceptance or rejection criteria to assess whether the machineries meet certain design demands. However, the existing design code *NEN 6786:2001 Rules for the design of movable bridges* defines a limit state design, meant for new machineries, which is based on simple linear spring-mass models. These models, as first proposed by Stroosma in 1980, are valid as long as damping is negligible and the externally applied loads, such as motor and braking torques, are assumed to be constant. However, observations show that these assumptions lead to a more stringent reassessment of existing bridges. As a result, existing bridge machineries do not confirm the model predictions and should unduly be replaced.

In fact, the powertrain of movable bridges are nonlinear systems consisting of many mechanical components, such as, couplings, shafts, gears and push-pull rods, with significant damping. Besides, the excitation of externally applied torques by motors and brakes are time-dependent and smooth.

In this paper, a model is developed that overcomes the limitations of the existing modelling approach. First, the classical semi-definite model is amended by an extra term which accounts for damping, using three load cases: opening from closed position, acceleration or deceleration and braking. The model gives an upper bound of the peak forces or torques occurring in the powertrain during normal operations and emergency braking. Subsequently, we discuss a novel nonlinear discrete model that allows one to deal with the time-dependency of the externally applied torques, such as, torque-speed characteristics of electric motors and braking torque characteristics.

Keywords: Movable bridge dynamics, bridge machinery, powertrain, electric motors and brakes

1 Introduction

The dynamic loads have hardly been involved in assessing the safe design of the bridge machineries in the distant past, so that one may be tempted to neglect its significance on movable bridges. However, this would be a premature judgment since the bridge machinery will undergo dynamic excitations due to external live loads such as wind, internal forces, inertia and gravity imbalance. Therefore, the engineers nowadays are usually advised to take the dynamic forces into account, as they are a significant component of the design loading and must be given primary consideration. Although, the machinery design starts with calculation of the decisive dynamic forces, that the bridge structure needs to resist or overcome in order to move, one cannot find overall mathematical models in the literature that is specifically used to determine the dynamic loads on bridge machineries.

Nevertheless, a significant progress was made in the Netherlands regarding the theoretical framework of movable bridge dynamics and its practical application when D. Stroosma proposed to use a simplified dynamic mass-spring model to determine the dynamic loads on the machinery parts during bridge operation in the eighties of the last century [1]. After identifying the various components, their physical properties and characteristics, Stroosma constructed a mathematical model of a torque regulated bridge machinery, which represents an idealisation of the actual physical system as shown in Figure (1). His model is a linear discrete-parameter system with two-degree-of-freedom (2-DOF), whose behaviour is described by a second-order differential equation in a rotating system.

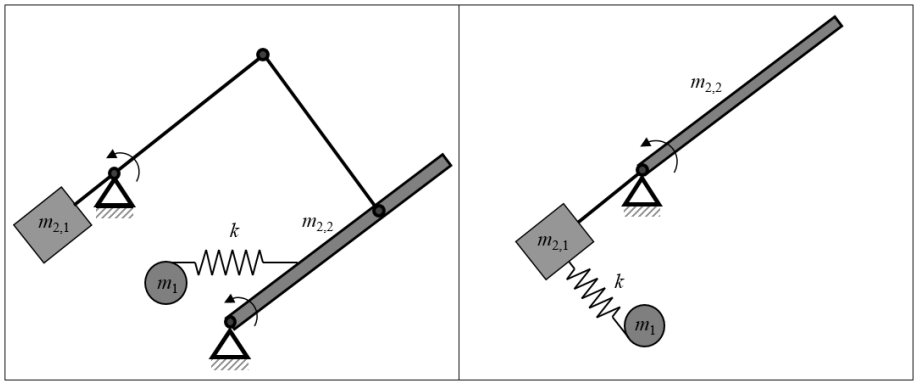

Figure 1. Dynamic model schematisations of a drawbridge (left) and a bascule bridge (right)

The first degree of freedom m_1 will represent the mass moment of inertia of the drive side of the system, which is the motor, and m_2 physically implies inertia of the driven side of the system, such as bridge decks and counterweights. k is the equivalent rotational stiffness of all connected parts of the powertrain, such as shafts, gears and couplings. Figure 2 shows a common way to make a diagram of this rotating system (left) and its equivalent translational system (right), These two systems and therefore the terms torque and forces will be used interchangeably in this paper.

For the first time, the Netherlands Standardisation Institute (*Nederlands Normalisatie Instituut, NEN*) issued certain calculation rules based on this model in 2001, which are implemented in the Dutch code for designing movable bridges, NEN 6786:2001 NL [2] with a supplement in 2002 (NEN 6786:2001/A1:2002 NL). NEN 6786 is updated in 2015 and led to the latest version in 2017 (NEN 6786:20017). Hence, nowadays NEN 6786 requires to take into account the dynamic forces and provides the user some simple analytical formulas. However, for the case of simplicity the damping ratio and the excitation by externally applied torques have not been modelled explicitly. The resulting deviations from the real world are considered as model uncertainties and in combination with other uncertainties accounted for by using semi-probabilistic partial factors. Therefore, the model does not fully incorporate the actual dynamic behaviour of the system. Since then, there has been no improvements proposed to his model.

In 1990 a vibration measurement is performed by TNO, the Netherlands Organisation for applied scientific research, on six bridges: four bascule and two drawbridges [5] in order to determine the damping of vibrations during bridge operation. Based on the measurements,

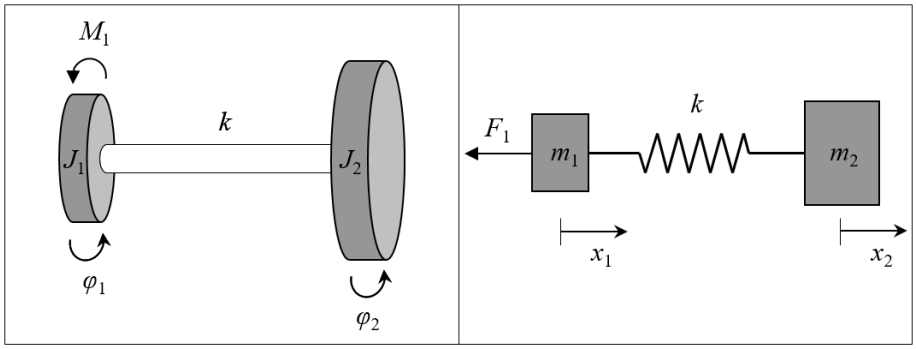

Figure 2. Dynamic model schematisations of a rotating system (left) and an equivalent translating system (right)

it is concluded that a bascule bridge without push-pull-rods, also known as ”spring buffers”, have a damping ratio of 0.4 to 0.7%. The measured bascule bridges with push-pull rods have a higher damping ratio from 2.5 to 6.0%. The measured damping ratio of drawbridges on the first natural frequency is greater than 10% and on the second natural frequency is approximately 2.0%. This has not led to any fundamental changes in the mathematical modelling of the bridge machineries or the calculation rules stated in the code, which are based on the same damping for all bridge types.

In this paper, the mathematical model of Stroosma is examined during starting, accelerating or decelerating and braking at full speed. Then an extension of the model is proposed to include damping effects and nonlinearity of externally applied excitations. A comparison between the results obtained from both models is also included. The governing equations in this paper are constructed methodically for easy implementation. The equations are suitable for e.g. the study of structural safety of torque regulated bridge machineries.

2 Undamped linear system with constant loads

In this section, the motor torque, which is opening the bridge from closed position, accelerating or decelerating it in an intermediate position, and the braking torque at a certain speed are approximated as a constant force. This approximation is based on the assumption that the externally applied forces are not depending on the displacements and velocities. Therefore, in this first step, our interest lies in the motion characteristics of a movable bridge and the response of the system to an action force, which is and remains constant. At $t = 0$, the system will go through some transient behaviour. This will be observed by vibrations occurring during the transient time until a steady state is reached. The constant force function $F(t)$ is depicted in Figure 3 and is defined mathematically as follows

$$F(t) = F \quad \text{for all} \quad t \tag{1}$$

2.1 Opening from closed position without damping

We begin by considering the horizontal vibration of the simple spring-mass system of Figure 4, which illustrates the undamped free vibration of the bridge opening from closed position. In the actual case, when the prime mover applies an acceleration force F_a , then,

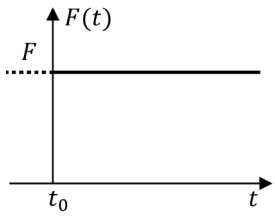

Figure 3. Constant force function

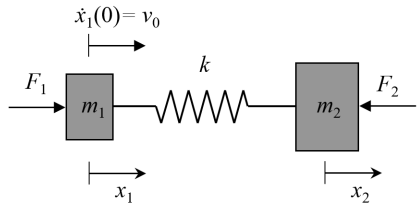

Figure 4. Opening from closed position with the static force included force, representing the wind load, the self-weight and variable deck weight of the bridge

due to the presence of clearances, an angle must first be cleared by the motor shaft m1 before being able to engage with the bridge m_2 . By that time, m_1 has already attained a velocity of v_0 . Thus v_0 is the initial velocity of the motor shaft and other components moving directly with it just before the bridge starts to move at time $t = t_0 = 0$ seconds. Furthermore, F_2 is the static force, representing the wind load, the self-weight and variable deck weight of the bridge. Therefore, F_2 corresponds to the force that must be generated to hold or move the bridge without acceleration. Obviously, F_1 is then the total force acting on m_1 , which refers to the force on the motor shaft due to acceleration or deceleration F_a , as well as the static force F_2 . Which means $F_1 = F_2 + F_a$. The direction of F_a depends on the closing or opening motion of the bridge deck. The initial conditions for the 2-DOF translational system at $t = 0$ are

$$\begin{aligned} x_1(0) &= 0 \\ x_2(0) &= -\frac{F_2}{k} \\ \dot{x}_1(0) &= v_0 \\ \dot{x}_2(0) &= 0 \end{aligned} \tag{2}$$

Then the equations of motion become

$$m_1\ddot{x}_1 + k(x_1 - x_2) = F_1 \tag{3}$$

$$m_2\ddot{x}_2 + k(x_2 - x_1) = -F_2 \tag{4}$$

Dividing by the masses and subtracting one equation from the other, gives

$$(\ddot{x}_2 - \ddot{x}_1) + (\frac{k}{m_1} + \frac{k}{m_2})(x_2 - x_1) = -\frac{F_1}{m_1} - \frac{F_2}{m_2} \tag{5}$$

the reduced system to a single-degree-of-freedom by substituting $x = x_2 - x_1$ gives

$$\ddot{x} + \omega^2 x = -\frac{F_1}{m_1} - \frac{F_2}{m_2} \tag{6}$$

where

$$\omega^2 = \frac{k}{m_1} + \frac{k}{m_2} \tag{7}$$

Then the initial conditions for $t = 0$ are

$$x(0) = x_2(0) - x_1(0) = -\frac{F_2}{k} \tag{8}$$

$$\dot{x}(0) = \dot{x}_2(0) - \dot{x}_1(0) = -v_0 \tag{9}$$

Introducing $\varepsilon = \frac{m_2}{m_1 + m_2}$, the general and particular solution of this differential equation becomes

$$x(t) = \frac{\varepsilon(F_1 - F_2)}{k}\cos(\omega t) - \frac{v_0}{\omega}\sin(\omega t) - \frac{\varepsilon F_1}{k} - \frac{(1-\varepsilon)F_2}{k} \tag{10}$$

Then the maximum spring force can be computed as

$$F_k(t) = \sqrt{(\varepsilon(F_1 - F_2))^2 + (-\frac{kv_0}{\omega})^2} + \varepsilon F_1 + (1-\varepsilon)F_2 \tag{11}$$

Simplification gives

$$F_k(t) = \sqrt{(\varepsilon(F_1 - F_2))^2 + (\frac{kv_0}{\omega})^2} + \varepsilon(F_1 - F_2) + F_2 \tag{12}$$

If the rotor of the motor is assumed to be clamped against vibrations by the magnetic field of the stator, m_1 can be taken very big, then ω as defined in Equation 7 becomes

$$\omega^2 = \frac{k}{m_2} \tag{13}$$

By substituting $F_a = F_1 - F_2$ and $\omega^2 = k/m_2$, this equation becomes the same as mentioned in NEN 6786:2001 [2] in case of opening from closed position, however, without the partial factors. However, when the initial displacement $x_2(0)$ is assumed to be zero, because the bridge in closed position is resting on its supports, then the maximum spring force after simplifications can be computed as

$$F_k(t) = \sqrt{(\varepsilon(F_1 - F_2) + F_2)^2 + (\frac{kv_0}{\omega})^2} + \varepsilon(F_1 - F_2) + F_2 \tag{14}$$

This results in a formula Equation 14, which is slightly different from Equation 12.

2.2 *Undamped vibration during accelerating or decelerating*

We consider a bridge that initially moves with a constant velocity v_0, then it undergoes a deceleration in intermediate positions under the influence of a force F_1. Since F_2 acting on

m_2 refers to the static load as mentioned in Section 2, it is assumed that F_2 remains unchanged in magnitude and direction. However, to this force, there is an opposed an equal reaction force on m_1 .

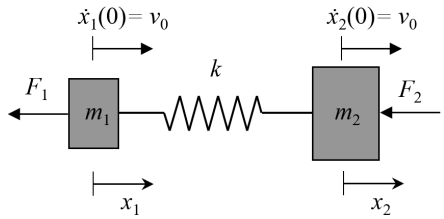

Figure 5. Decelerating the bridge from a constant speed, while opening $F_1 = F_a - F_2$ *. Note that the velocity* v_0 *during this stage is the nominal speed of the motor, which is not the value* v_0 *when starting the bridge.*

The effect of F_2 can be accounted for by including it into the initial conditions. This results into the following initial conditions for the system.

$$\begin{aligned} x_1(0) &= 0 \\ x_2(0) &= -\frac{F_2}{k} \\ \dot{x}_1(0) &= v_0 \\ \dot{x}_2(0) &= v_0 \end{aligned} \tag{15}$$

Defining $x = x_2 - x_1$, the system can be reduced to a single-degree-of-freedom as follows

$$\ddot{x} + \omega^2 x = \frac{F_1}{m_1} - \frac{F_2}{m_2} \tag{16}$$

Note that the dynamics of this system would be exactly the same as when the bridge starts from rest at open position and closes with a constant acceleration under the influence of a force F_1 . Because when the bridge is at rest, then $\dot{x}_2(0) - \dot{x}_1(0) = 0$, which implies the same result for the initial condition regarding the velocity. The equilibrium position of the system is when x = 0. Then the general form of the solution becomes

$$x(t) = A\cos(\omega t) + B\sin(\omega t) + C \tag{17}$$

where C is the particular solution and it is found as follows

$$C = \frac{\frac{F_1}{m_1} - \frac{F_2}{m_2}}{\frac{k}{m_1} + \frac{k}{m_2}} = \frac{F_1}{k}\frac{m_2}{m_1 + m_2} + \frac{F_2}{k}\frac{m_2}{m_1 + m_2} - \frac{F_2}{k} \tag{18}$$

Coefficient A can be found using Equation 17 and the initial conditions. Coefficient $B = 0$ and can be found from the derivative of Equation 17 and the initial conditions. Substituting $\varepsilon = \frac{m_2}{m_1 + m_2}$, A, B and C and after rearrangement of the terms, then the solution becomes

$$x(t) = (-\frac{F_1}{k}\varepsilon - \frac{F_2}{k}\varepsilon)\cos(\omega t) + (\frac{F_1}{k}\varepsilon + \frac{F_2}{k}\varepsilon - \frac{F_2}{k}) \tag{19}$$

The force acting on the spring is computed as $F_k(t) = kx(t)$. Then $F_k(t)$ becomes

$$F_k(t) = -(F_1 + F_2)\varepsilon\cos(\omega t) + (F_1 + F_2)\varepsilon - F_2 \tag{20}$$

Therefore, Equation 20 can be written as

$$F_k(t) = \varepsilon F_1(1 - \cos(\omega t)) + \varepsilon F_2(1 - \cos(\omega t)) - F_2 \tag{21}$$

The maximum value of the spring force $F_{k\max}$ during opening can be derived from Equation 21.

$$F_{k\max}^{open} = 2\varepsilon F_1 + 2\varepsilon F_2 - F_2 \tag{22}$$

As mentioned before, F_1 is the total force that causes acceleration or deceleration in the system and F_2 refers to the static load due to self-weight, wind and variable deck weight. Therefore, F_1 is consisting of two forces, a force as high as the static force F_2 plus a force, which is the dynamic contribution F_a to accelerate or decelerate the system, when it is respectively, in rest or has a constant velocity. In case of decelerating while opening the bridge $F_1 = F_a - F_2$. Substitution into Equation 21 gives

$$F_k(t) = \varepsilon F_a(1 - \cos(\omega t)) - F_2 \tag{23}$$

This is the case whenever the force F_1 acts on the same direction of the static force F_2 . Hence, for the maximum load on the prime mover we obtain

$$F_{k\max}^{open} = 2\varepsilon F_a - F_2 \tag{24}$$

Following the same methodology for the closing situation, the equation for the maximum spring force $F_{k\max}$ becomes

$$F_{k\max}^{close} = -2\varepsilon F_1 + 2\varepsilon F_2 - F_2 \tag{25}$$

This will be the case, whenever the force F_1 acts on the opposite direction of the static force F_2 . In case of decelerating the bridge while closing $F_1 = F_2 + F_a$ and substitution gives

$$F_{k\max}^{close} = -2\varepsilon(F_a + F_2) + 2\varepsilon F_2 - F_2 = -2\varepsilon F_a - F_2 \tag{26}$$

Note that the dynamics of this system would be exactly the same as when the bridge starts from rest at closed position and opens with a constant acceleration under the influence of a force F_1. Combining both Equation 24 and 26 gives an absolute maximum value for the spring force

$$\left|F_{k\max}\right| = 2\varepsilon\left|F_a\right| + F_2 \tag{27}$$

2.3 *Undamped vibration during braking at full speed*

The process of braking is the same as decelerating the system. Therefore, the system in Section 2 also applies for this case, if we replace F_1 by F_{br}. Hence, in order to analyse this load combination by the application of brakes, we use a system shown in Figure 6 which is equivalent to Figure 5.

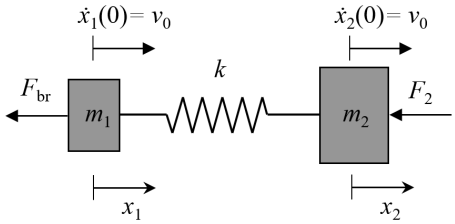

Figure 6. Braking the system from a constant speed, while opening $F_{br} = F_a - F_2$

This load situation refers to an uncontrolled emergency stop by means of mechanical brakes. Again, we write the same initial conditions as stated in Equation 15, including the effect of the static load. The force acting in the spring is then obtained to be equal to Equation 23. This is the case whenever the braking force F_{br} acts on the same direction of the static force F_2. Therefore, substitution of F_1 by F_{br} gives

$$F_k(t) = \varepsilon F_{br}(1 - \cos(\omega t)) + \varepsilon F_2(1 - \cos(\omega t)) - F_2 \tag{28}$$

The maximum value is given as

$$F_{k\max}^{open} = 2\varepsilon F_{br} + 2\varepsilon F_2 - F_2 \tag{29}$$

On reversing the direction of the velocity, we get a braking force F_{br} in the opposite direction of the static force F_2 as follows

$$F_{k\max}^{close} = -2\varepsilon F_{br} + 2\varepsilon F_2 - F_2 \tag{30}$$

Equation 30 can be multiplied by −1 in order to get a positive value for the F_{br} . Then the equation becomes

$$F_{k\max}^{close} = 2\varepsilon F_{br} - 2\varepsilon F_2 + F_2 \tag{31}$$

The maximum absolute value of $F_{k\max}$ for both situations can be combined in one equation as follows

$$\left|F_{k\max}\right| = 2\varepsilon F_{br} + F_2\left|1-2\varepsilon\right| \tag{32}$$

Note that the braking force is not constant, because it is in fact a friction force. After the motor shaft comes to a standstill due to application of the braking force, then the braking force will act as a reaction force holding the shaft against any further rotation, till the deck comes to a standstill as well.

3 Linear systems with damping

3.1 Opening from closed position with viscous damping

The system of Figure 7 illustrates the damped free vibration of a linear system opening from closed position including a damper. As mentioned earlier, F_2 corresponds to the force that must be generated to hold or move the bridge without acceleration and F_1 is the total force acting on m_1 , which refers to the acceleration or deceleration force together with the static force. Variable c is the damping constant and the other variables are the same as described in Section 2. The initial conditions at t = 0 are

$$x(0) = x_2(0) - x_1(0) = -\frac{F_2}{k} \tag{33}$$

$$\dot{x}(0) = \dot{x}_2(0) - \dot{x}_1(0) = -v_0 \tag{34}$$

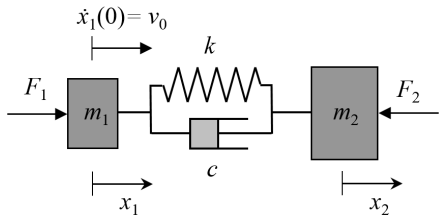

Figure 7. Opening from closed position with damping $F_1 = F_a + F_2$

Then the equations of motion become

$$m_1\ddot{x}_1 + c(\dot{x}_1 - \dot{x}_2) + k(x_1 - x_2) = F_1 \tag{35}$$

$$m_2\ddot{x}_2 + c(\dot{x}_2 - \dot{x}_1) + k(x_2 - x_1) = -F_2 \tag{36}$$

Dividing by the masses and subtracting one equation from the other, gives

$$(\ddot{x}_2 - \ddot{x}_1) + (\frac{c}{m_1} + \frac{c}{m_2})(\dot{x}_2 - \dot{x}_1) + (\frac{k}{m_1} + \frac{k}{m_2})(x_2 - x_1) = -\frac{F_1}{m_1} - \frac{F_2}{m_2} \tag{37}$$

The reduced system to a single-degree-of-freedom by substituting $x = x_2 - x_1$ gives

$$\ddot{x} + 2\zeta\omega\dot{x} + \omega^2 x = -\frac{F_1}{m_1} - \frac{F_2}{m_2} \tag{38}$$

where

$$2\zeta\omega = \frac{c}{m_1} + \frac{c}{m_2} \tag{39}$$

$$\omega = \sqrt{\frac{k}{m_1} + \frac{k}{m_2}} \qquad (\omega \in \mathbb{R}) \tag{40}$$

Solving this ordinary differential equation with the given initial conditions gives the following solution

$$\begin{aligned} x(t) = {} & \frac{e^{(-\zeta+\sqrt{\zeta^2-1})\omega t}}{2\sqrt{\zeta^2-1}\omega^2 k m_1 m_2}\left(-v_0\omega k m_1 m_2 + \left(\zeta+\sqrt{\zeta^2-1}\right)F_1 k m_2 + \left(\zeta+\sqrt{\zeta^2-1}\right)F_2 m_1(k-\omega^2 m_2)\right) + \\ & + \frac{e^{-(\zeta+\sqrt{\zeta^2-1})\omega t}}{2\sqrt{\zeta^2-1}\omega^2 k m_1 m_2}\left(v_0\omega k m_1 m_2 + \left(-\zeta+\sqrt{\zeta^2-1}\right)F_1 k m_2 + \left(-\zeta+\sqrt{\zeta^2-1}\right)F_2 m_1(k-\omega^2 m_2)\right) - \\ & - \frac{F_1 m_2 + F_2 m_1}{\omega^2 m_1 m_2} \end{aligned} \tag{41}$$

By substituting $\omega^2 = k\frac{m_1+m_2}{m_1 m_2}$ the expression $k - \omega^2 m_2$ becomes $-k\frac{m_2}{m_1}$. Simplifying Equation 41 gives

$$\begin{aligned} x(t) = {} & \frac{e^{(-\zeta+\sqrt{\zeta^2-1})\omega t}}{2\sqrt{\zeta^2-1}k^2(m_1+m_2)}\left(-v_0\omega k m_1 m_2 + \left(\zeta+\sqrt{\zeta^2-1}\right)F_1 k m_2 - \left(\zeta+\sqrt{\zeta^2-1}\right)F_2 k m_1\right) + \\ & + \frac{e^{-(\zeta+\sqrt{\zeta^2-1})\omega t}}{2\sqrt{\zeta^2-1}\omega^2 k m_1 m_2}\left(v_0\omega k m_1 m_2 + \left(-\zeta+\sqrt{\zeta^2-1}\right)F_1 k m_2 - \left(-\zeta+\sqrt{\zeta^2-1}\right)F_2 m_2\right) - \\ & - \frac{F_1 m_2 + F_2 m_1}{k(m_1+m_2)} \end{aligned} \tag{42}$$

Using the expressions $F_a = F_1 - F_2$, $e^{xi} = \cos(x) + i\sin(x)$ and $\sqrt{\zeta^2-1} = i\sqrt{1-\zeta^2}$, because $\zeta < 1$, Equation 42 can be simplified as

$$\begin{aligned} x(t) = {} & \frac{e^{-\zeta\omega t}\left(-v_0\omega m_1 m_2 + \zeta F_a m_2\right)\sin(\sqrt{1-\zeta^2}\omega t)}{\sqrt{1-\zeta^2}k(m_1+m_2)} + \frac{e^{-\zeta\omega t}\sqrt{1-\zeta^2}F_a m_2\cos(\sqrt{1-\zeta^2}\omega t)}{\sqrt{1-\zeta^2}k(m_1+m_2)} - \\ & - \frac{F_a m_2}{k(m_1+m_2)} - \frac{F_2}{k} \end{aligned} \tag{43}$$

Using the expression $\varepsilon = \frac{m_2}{m_1+m_2}$ Equation 43 can be further simplified as

$$x(t) = e^{-\zeta\omega t}\sin(\sqrt{1-\zeta^2}\,\omega t)\frac{\varepsilon(-v_0\omega m_1 + \zeta F_a)}{\sqrt{1-\zeta^2}\,k} + e^{-\zeta\omega t}\cos(\sqrt{1-\zeta^2}\,\omega t)\frac{\varepsilon F_a}{k} - \frac{\varepsilon F_a}{k} - \frac{F_2}{k} \tag{44}$$

The force in the system is the sum of the forces in the spring and the damper $F_k(t) = kx(t) + c\dot{x}(t)$. However, the force in the damper, compared to the spring force, is negligible, due to a combination of small velocities of the bridge and small damping ratio ζ , which is usually smaller than 10%. Therefore, our interest lies in determining the dynamic amplification factor inside the term $kx(t)$ as a function of the damping ratio ζ , while $c\dot{x}(t)$ is ignored. Then the spring force $F_k(t) = kx(t)$ becomes

$$F_k(t) = e^{-\zeta\omega t}\sin(\sqrt{1-\zeta^2}\,\omega t)\frac{\varepsilon(-v_0\omega m_1 + \zeta F_a)}{\sqrt{1-\zeta^2}} + e^{-\zeta\omega t}\cos(\sqrt{1-\zeta^2}\,\omega t)\varepsilon F_a - \varepsilon F_a - F_2 \tag{45}$$

We can now determine the time $t_{\max}$, when the force is at its maximum, by solving $\frac{d}{dt}F_k(t) = 0$ for the time t

$$t_{\max} = \frac{\arctan\dfrac{\sqrt{1-\zeta^2}\,kv_0}{\zeta kv_0 - \omega\varepsilon F_a}}{\sqrt{1-\zeta^2}\,\omega} \tag{46}$$

By substituting $t_{\max}$ in Equation 45 and simplifying, we find for the maximum force

$$F_{k\max} = e^{Z}\sqrt{(\varepsilon F_a)^2 + \left(\frac{kv_0}{\omega}\right)^2 - \frac{2\zeta kv_0\varepsilon F_a}{\omega}} + \varepsilon F_a + F_2 \tag{47}$$

where

$$Z = \frac{\zeta\arctan\dfrac{\sqrt{1-\zeta^2}\,kv_0}{\omega\varepsilon F_a - \zeta kv_0}}{\sqrt{1-\zeta^2}} \tag{48}$$

Z should be negative, meaning $\arctan\dfrac{\sqrt{1-\zeta^2}\,kv_0}{\omega\varepsilon F_a - \zeta kv_0} < 0$, otherwise

$$Z = \frac{\zeta}{\sqrt{1-\zeta^2}}\left(-\pi + \arctan\frac{\sqrt{1-\zeta^2}\,kv_0}{\omega\varepsilon F_a - \zeta kv_0}\right) \tag{49}$$

According to the literature, the damping ratio ζ is usually smaller than 10%. Therefore, ζ^2 is very small, leading to

$$\sqrt{1-\zeta^2} \approx 1 \tag{50}$$

Moreover, the rotor shaft is rotating inside the magnetic field of the stator, therefore, we may assume that free vibration of the rotor is not possible as mentioned in [1]. As a result, when calculating the torsional frequency of the system as mentioned in Equation 40, we may assume m_1 is very big. Therefore, ω becomes

$$\omega = \sqrt{\frac{k}{m_2}} \tag{51}$$

Substituting Equation 49, 50 and 51 into Equation 47 gives

$$F_{k\max} = e^{\zeta\left(-\pi+\arctan\frac{kv_0}{\omega\varepsilon F_a-\zeta k v_0}\right)}\sqrt{(\varepsilon F_a)^2+km_2v_0^2-2\zeta v_0\varepsilon F_a\sqrt{km_2}}+\varepsilon F_a+F_2 \tag{52}$$

This equation can be approached by a simpler formula as the square root can be approximated

$$F_{k\max} \approx e^{\zeta\left(-\pi+\arctan\frac{kv_0}{\omega\varepsilon F_a-\zeta k v_0}\right)}\left(\varepsilon F_a+\zeta\sqrt{km_2}v_0\right)+\varepsilon F_a+F_2 \tag{53}$$

If v_0 is very small ($v_0 \to 0$), then Equation 52 reduces to

$$\left|F_{k\max}\right| = (1+e^{-\pi\zeta})\varepsilon\left|F_a\right|+F_2 \tag{54}$$

The expression $(1+e^{-\pi\zeta})$ is the dynamic amplification factor as a function of ζ , which is equal to 2 as shown in previous section, if ζ = 0.

3.2 Damped vibration during accelerating or decelerating

Following the same methodology for the opening situation with damping as shown in Figure 7, in Figure 8 we consider a bridge that initially moves with a constant velocity v_0 , then it undergoes a deceleration in intermediate positions under the influence of a force F_1 . The effect of F_2 can be accounted for by including it into the initial conditions. This results into the same initial conditions of Equation 15. Taking damping into account, the equations of motion become

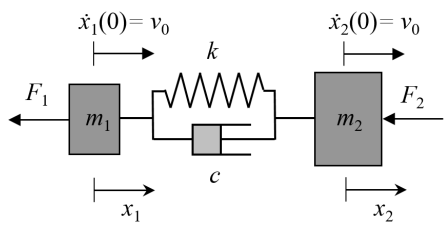

Figure 8. Decelerating the bridge from a constant speed, while opening $F_1 = F_a - F_2$

$$m_1\ddot{x}_1 + c(\dot{x}_1 - \dot{x}_2) + k(x_1 - x_2) = -F_1 \tag{55}$$

$$m_2\ddot{x}_2 + c(\dot{x}_2 - \dot{x}_1) + k(x_2 - x_1) = -F_2 \tag{56}$$

The reduced system to a single-degree-of-freedom by substituting $x = x_2 - x_1$ gives

$$\ddot{x} + 2\zeta\omega\dot{x} + \omega^2 x = \frac{F_1}{m_1} - \frac{F_2}{m_2} \tag{57}$$

where $2\zeta\omega$ and ω^2 are defined in Equation 39 and 7. The initial conditions for t = 0 remain

$$x(0) = x_2(0) - x_1(0) = -\frac{F_2}{k} \tag{58}$$

$$\dot{x}(0) = \dot{x}_2(0) - \dot{x}_1(0) = 0 \tag{59}$$

Solving Equation 57 with the given initial conditions gives the following solution

$$\begin{aligned} x(t) = {} & \frac{e^{(-\zeta+\sqrt{\zeta^2-1})\omega t}}{2(\zeta^2-1)\omega^2 k m_1 m_2}\left(\zeta\sqrt{\zeta^2-1}+\zeta^2-1\right)\left(F_1 k m_2 - F_2 k m_1 + \omega^2 F_2 m_1 m_2\right) - \\ & - \frac{e^{-(\zeta+\sqrt{\zeta^2-1})\omega t}}{2(\zeta^2-1)\omega^2 k m_1 m_2}\left(-\zeta\sqrt{\zeta^2-1}+\zeta^2-1\right)\left(F_1 k m_2 - F_2 k m_1 + \omega^2 F_2 m_1 m_2\right)) + \\ & + \frac{F_1 m_2 - F_2 m_1}{\omega^2 m_1 m_2} \end{aligned} \tag{60}$$

Using the expression $e^{ix} = \cos(x) + i\sin(x)$, $\omega^2 = k\frac{m_1 + m_2}{m_1 m_2}$, $F_1 = F_a - F_2$ and

$\sqrt{\zeta^2 - 1} = i\sqrt{1-\zeta^2}$ because $\zeta < 1$, Equation 60 can be simplified as

$$x(t) = -\frac{e^{-\zeta\omega t} F_a m_2 \cos(\sqrt{1-\zeta^2}\,\omega t)}{k(m_1 + m_2)} + \frac{e^{-\zeta\omega t}\zeta F_a m_2 \sqrt{1-\zeta^2}\sin(\sqrt{1-\zeta^2}\,\omega t)}{k(\zeta^2-1)(m_1+m_2)} + \frac{(F_a - F_2)m_2 - F_2 m_1}{k(m_1+m_2)} \tag{61}$$

Substitution of $\varepsilon = \frac{m_2}{m_1 + m_2}$ gives for the maximum spring force $F_k(t) = kx(t)$

$$F_k(t) = e^{-\zeta\omega t}\left(-\varepsilon F_a \cos(\sqrt{1-\zeta^2}\,\omega t) - \frac{\varepsilon F_a \zeta \sin(\sqrt{1-\zeta^2}\,\omega t)}{\sqrt{1-\zeta^2}}\right) + \varepsilon F_a - F_2 \tag{62}$$

Substituting ζ = 0 gives back Equation 23 without damping as mentioned in Section 2. Using the expression $b_1\sin(x) + b_2\cos(x) = \text{sign}(b_1)\sqrt{b_1^2 + b_2^2}\sin(x + \arctan\frac{b_2}{b_1})$, then the above formula can be simplified as

$$F_k(t) = e^{-\zeta\omega t}\varepsilon F_a\left(-\frac{1}{\sqrt{1-\zeta^2}}\sin\left(\sqrt{1-\zeta^2}\,\omega t + \arctan\frac{\sqrt{1-\zeta^2}}{\zeta}\right)\right) + \varepsilon F_a - F_2 \tag{63}$$

We can now determine the time $t_{\max}$, when the force is at its maximum, by solving

$\frac{d}{dt}F_k(t) = 0$ for the time t

$$\frac{d}{dt}F_k(t) = e^{-\zeta\omega t}\frac{\zeta\varepsilon F_a\omega\sin\left(\sqrt{1-\zeta^2}\omega t + \arctan\frac{\sqrt{1-\zeta^2}}{\zeta}\right)}{\sqrt{1-\zeta^2}} - \\ - e^{-\zeta\omega t}\varepsilon F_a\omega\cos\left(\sqrt{1-\zeta^2}\omega t + \arctan\frac{\sqrt{1-\zeta^2}}{\zeta}\right) = 0 \tag{64}$$

Because $e^{-\zeta\omega t}\varepsilon F_a\omega \neq 0$, therefore

$$\frac{\zeta\sin\left(\sqrt{1-\zeta^2}\omega t + \arctan\frac{\sqrt{1-\zeta^2}}{\zeta}\right)}{\sqrt{1-\zeta^2}} - \cos\left(\sqrt{1-\zeta^2}\omega t + \arctan\frac{\sqrt{1-\zeta^2}}{\zeta}\right) = 0$$

$$\tan\left(\sqrt{1-\zeta^2}\omega t + \arctan\frac{\sqrt{1-\zeta^2}}{\zeta}\right) = \frac{\sqrt{1-\zeta^2}}{\zeta} \tag{65}$$

$$\sqrt{1-\zeta^2}\omega t + \arctan\frac{\sqrt{1-\zeta^2}}{\zeta} = \arctan\frac{\sqrt{1-\zeta^2}}{\zeta} + n\pi$$

$$t = \frac{n\pi}{\sqrt{1-\zeta^2}\omega}$$

Where n = 0, 1, 2, 3, … For each value of n, there is a local maximum (or minimum, when the sign is negative). However, in this case the global maximum (or minimum) of the force will be at n = 1, therefore

$$t_{\max} = \frac{\pi}{\sqrt{1-\zeta^2}\omega} \tag{66}$$

By substituting $t_{\max}$ in Equation 62 and simplifying we find for the maximum force

$$F_{k\max}^{open} = e^{-\frac{\pi\zeta}{\sqrt{1-\zeta^2}}}\varepsilon F_a + \varepsilon F_a - F_2 \tag{67}$$

Note that in this opening case $F_1 = F_a - F_2$ and therefore $F_a = F_1 + F_2$. However, if we follow the same methodology in case of closing the bridge, we obtain

$$F_{k\max}^{close} = e^{-\frac{\pi\zeta}{\sqrt{1-\zeta^2}}}\varepsilon F_a + \varepsilon F_a + F_2 \tag{68}$$

In this closing case $F_1 = F_a + F_2$ and therefore $F_a = F_1 - F_2$. The maximum absolute value of the force acting on the bridge despite the direction of the movement can be found by combining Equation 67 and 68 as follows

$$|F_{k\max}| = (1 + e^{-\frac{\pi\zeta}{\sqrt{1-\zeta^2}}})\varepsilon|F_a| + |F_2| \tag{69}$$

If $\zeta^2 \to 0$, then this equation can be simplified further as

$$|F_{k\max}| = (1 + e^{-\pi\zeta})\varepsilon|F_a| + |F_2| \tag{70}$$

Note that the Equation 70 is the same as Equation 54.

3.3 Damped vibration during braking at full speed

The system of Figure 9 can be regarded as an idealised mathematical model of a movable bridge, while braking by a constant braking force F_{br} from a constant speed v_0 and taking into account damping in the powertrain. Note that this system is the same as previous one, when we replace F_1 by F_{br}. Hence, in order to analyse this load combination by the application of brakes, we use the equivalent system of previous section. The maximum value of the force acting on the bridge during opening can be found from Equation 67. Substitution of $F_a = F_{br} + F_2$ gives

$$F_{k\max}^{open} = e^{-\frac{\pi\zeta}{\sqrt{1-\zeta^2}}}\varepsilon(F_{br} + F_2) + \varepsilon(F_{br} + F_2) - F_2 \tag{71}$$

Simplification gives

$$F_{k\max}^{open} = (1 + e^{-\frac{\pi\zeta}{\sqrt{1-\zeta^2}}})\varepsilon F_{br} + (1 + e^{-\frac{\pi\zeta}{\sqrt{1-\zeta^2}}})\varepsilon F_2 - F_2 \tag{72}$$

On reversing the direction of the velocity in case of braking while closing the bridge, we get a braking force F_{br} in the opposite direction of the static force F_2. Then the maximum value of the force acting on the bridge during closing can be found from Equation 68. Substitution of $F_a = F_{br} - F_2$ gives

$$F_{k\max}^{close} = -e^{-\frac{\pi\zeta}{\sqrt{1-\zeta^2}}}\varepsilon(F_{br} - F_2) - \varepsilon(F_{br} - F_2) - F_2 \tag{73}$$

Simplification gives

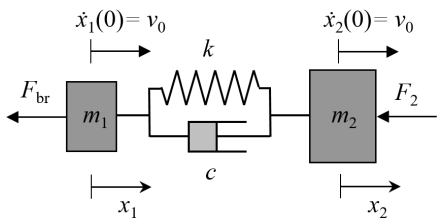

Figure 9. Braking the damped system from a constant speed, while opening $F_{br} = F_a - F_2$

$$F_{k\max}^{close} = -(1+e^{-\frac{\pi\zeta}{\sqrt{1-\zeta^2}}})\varepsilon F_{br} + (1+e^{-\frac{\pi\zeta}{\sqrt{1-\zeta^2}}})\varepsilon F_2 - F_2 \tag{74}$$

The maximum absolute value of $F_{k\max}$ of both situations can be combined in one equation as follows

$$\left|F_{k\max}\right| = (1+e^{-\frac{\pi\zeta}{\sqrt{1-\zeta^2}}})\varepsilon F_{br} + F_2 \,|\, 1-(1+e^{-\frac{\pi\zeta}{\sqrt{1-\zeta^2}}})\varepsilon \,| \tag{75}$$

If $\zeta^2 \to 0$, then this equation can be simplified further as

$$\left|F_{k\max}\right| = (1+e^{-\pi\zeta})\varepsilon F_{br} + F_2 \left|1-(1+e^{-\pi\zeta})\varepsilon\right| \tag{76}$$

Note that the Equation 76 is the same as Equation 70 if F_{br} is replaced by $F_a - F_2$.

4 The effect of damping ratio on dynamic amplification factor

In this section, the effect of damping ratio ζ on the dynamic amplification factor Φ_a is investigated. As introduced by the code NEN 6786:2001 [2], Φ_a is taken as a constant for all bridge types Φ_a = 1.9. In Section 2 and more specifically in Equation 27 is shown that, if damping is not taken into account, this value should theoretically be 2.0. However, in case of a damped system as shown in Equation 70, Φ_a is a function of the damping ratio, according to the following equation

$$\Phi_a(\zeta) = 1 + e^{-\frac{\pi\zeta}{\sqrt{1-\zeta^2}}} \tag{77}$$

where $\sqrt{1-\zeta^2} \approx 1$ for all $\zeta < 0.1$. Therefore, we introduce Φ_ζ , which is depicted in Figure 10 and defined mathematically as follows

$$\Phi_\zeta = \Phi_a(\zeta) \approx 1 + e^{-\pi\zeta} \tag{78}$$

In contrast to the code, inserting a different damping ratio into Equation 78 for different bridge types, as mentioned in [5], we obtain various amplification factors for each situation as shown in Table 1, depending on the value of ζ .

5 Comparison with calculation rules from NEN 6786

The calculation rules to compute dynamic forces in movable bridge machineries according to NEN 6786:2017, are based on an undamped dynamic model. However, if the damped model is considered by using a spring-damper-mass system, as mentioned earlier in this paper, then the damping effects on the calculation rules is directly included in the calculation rules depending on a given damping ratio ζ. In Table 2 the differences between the calculated maximum dynamic forces in case of an undamped and damped system are summarised for three load situations.

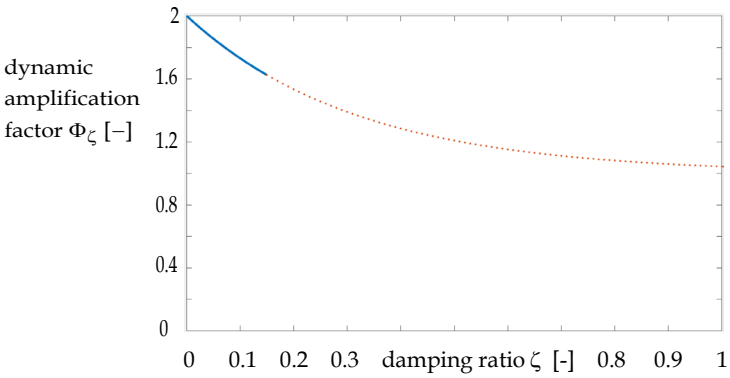

Figure 10. Dynamic amplification factor as a function of damping ratio

Table 1. Damping-dependent dynamic amplification factor Φ_ζ for different cases based on measurements mentioned in [5]

Description	ζ [-]	Φ_ζ
Model without damping	0.0%	2.0
Bascule bridges without push-pull rods	0.4 - 0.7%	1.99 - 1.98
According to NEN 6786, when Φ_a = 1.9	3.35%	1.9
Average default value in this paper	5.0%	1.85
Bascule bridges with push-pull rods	2.5 - 6.0%	1.92 - 1.83
Drawbridges	10.0%	1.73

6 Models with torque-speed dependent characteristics

In section 2 and 3, we mentioned the response to a constant load F_1. The question remains as to how obtain the response to a more realistic arbitrary excitation under the action of a force $F(\dot{x})$, which is a given function of the velocity $\dot{x}$. In coming sections, we consider the motor and brake torques as varying force excitations. On one hand, we distinguish the speed-torque characteristics of a squirrel *cage motor* $F_{sc}(\dot{x})$ and a *slip ring* $F_{sr}(\dot{x})$ motor, and on the other hand, we consider the characterisation of an *emergency stop* braking torque $F_{br}(\dot{x})$ as a function of the speed. $F_{sc}(\dot{x})$, $F_{sr}(\dot{x})$ and $F_{br}(\dot{x})$ will be used to replace the constant force F_1 in the previous sections.

Table 2. Comparison of given calculation rules to compute dynamic forces in movable bridge machineries according to NEN 6786:2017, with a damped rotational semidefinite system. If $\omega_0 \to 0$, then Equation 70 may be used to compute the dynamic loads during opening from closed position instead of Equation 53.

Load situations	Calculations rules NEN 6786-1:2017	Proposed model with damping	Equivalent translating system
Opening from closed position	$M_2 + \varepsilon M_a + 0.9\sqrt{(\varepsilon M_a)^2 + kJ_2\omega_0^2}$	$M_2 + \varepsilon M_a + e^Z(\varepsilon M_a + \zeta\omega_0\sqrt{kJ_2})$	Eq. 53
Accelerating or decelerating	$\Phi_a\varepsilon(M_2 + M_a) + \lvert 1 - \Phi_a\varepsilon \rvert M_2$	$\lvert M_2 \rvert + \Phi_\zeta\varepsilon\lvert M_a \rvert$	Eq. 70
Braking at full speed	$\Phi_a\varepsilon M_{br} + \lvert 1 - \Phi_a\varepsilon \rvert M_2$	$\Phi_\zeta\varepsilon M_{br} + \lvert 1 - \Phi_\zeta\varepsilon \rvert M_2$	Eq. 76

$$Z = \zeta\left(\arctan\frac{k\omega_0}{\omega\varepsilon M_a - \zeta k\omega_0}\right) \quad \text{if} \quad \arctan\frac{k\omega_0}{\omega\varepsilon M_a - \zeta k\omega_0} < 0$$

$$Z = \zeta\left(-\pi + \arctan\frac{k\omega_0}{\omega\varepsilon M_a - \zeta k\omega_0}\right) \quad \text{otherwise}$$

$$\Phi_\zeta = 1 + e^{-\pi\zeta}$$

$$\omega = \sqrt{\frac{k}{J_2}}$$

In fact, $\omega = \sqrt{\frac{k}{J_1} + \frac{k}{J_2}}$, however, as assumed in [1], free vibration of the rotor m_1 in the magnetic field of the stator is negligible. Therefore, m_1 is considered to be very big, when calculating ω. The notations according to Tabel 11 of NEN 6786:2017 [3] are $M_{br} = M_{br,Ed}$, $M_2 = M_{Ed}$, $M_a = M_{a,Ed}$, $J_2 = I_2$, $k = C_1$ and $\omega_0 = \omega$.

6.1 *Modelling with a squirrel cage motor*

In this subsection we consider a movable bridge driven by a squirrel cage motor. Figure 11 is a typical speed-torque characteristics of a squirrel cage motor. Variable s_0 is the slip at t = 0, while the $\dot{x}_1(0) = v_0$. Variable s_b is the break down slip and s_{ns} is slip at the moment the motor reaches its nominal speed. The slip s is defined as one minus the ratio between the shaft rotation speed $\dot{x}_1$ and the nominal speed $\dot{x}_{ns}$ as follows

$$s = 1 - \frac{\dot{x}_1}{\dot{x}_{ns}} \tag{79}$$

where $\dot{x}_{ns}$ is the nominal speed of the motor at which the motor delivers the nominal torque. The motor is the most efficient at that point. This curve can analytically be approached as described in [4] by Equation 80.

$$F_{sc}(s) = \frac{bs}{s^2 + a_1 s + a_0} \tag{80}$$

If the rotor is not turning and starts to rotate, then the slip is 100%. This is the first operating point, with the starting torque F_{st} , which is called the *lock-rotor torque*. At this point, the motor current is at maximum. Slip and motor current are reduced, when the rotor begins turning. We can use this point in order to determine b as follows

$$F_{st} = F_{sc}(1) = \frac{bs}{s^2 + a_1 s + a_0} \tag{81}$$

It can be seen from Equation 80 that the coefficient b is given by

$$b = F_{st}(1 + a_1 + a_0) \tag{82}$$

We can use a second operating point, which relates to the break-down force, in order to find a_1 and a_0 . At this maximum force condition, the derivative of the force in Equation 80

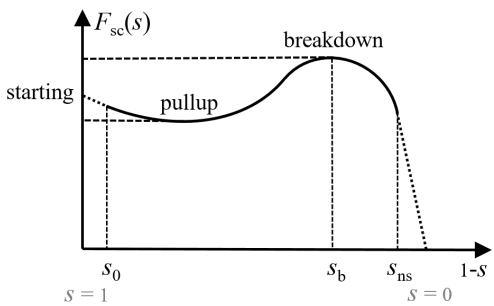

Figure 11. Force-slip curve of a squirrel cage motor $F_{cs}(s)$. The driving force of the motor is the motor torque.

with respect to slip should be zero and is given by

$$\frac{dF_{sc}(s)}{ds} = \frac{b(a_0 - s^2)}{(s^2 + a_1 s + a_0)^2} = 0 \tag{83}$$

Substituting $s = s_b$ gives

$$\frac{b(a_0 - s_b^2)}{(s_b^2 + a_1 s_b + a_0)^2} = 0 \tag{84}$$

Equation 84 shows that when $\frac{dF_{sc}(s)}{ds} = 0$ and $s = s_b$, the coefficient $a_0 = s_b^2$, where a_0 is related to the break-down slip s_b.

$$a_0 = s_b^2 \tag{85}$$

Hence, the break down force is rewritten by making use of Equation 85 as

$$F_{bd} = \frac{b}{2s_b + a_1} \tag{86}$$

Substituting Equation 85 into Equation 80, and equating $F_{sc}(s_b)$ and F_{bd}, then a_1 is solved by

$$a_1 = \frac{F_{st}(1 + s_b^2) - 2F_{bd}s_b}{F_{bd} - F_{st}} \tag{87}$$

Substitution of Equation 79, 82, 85, 87 into Equation 80 gives $F_{sc}(s)$, which is equivalent to $F_{sc}(\dot{x}_1)$.

$$F_{sc}(\dot{x}_1) \leftrightarrow F_{sc}(x_1) = \frac{F_{st}\left(1 + \frac{F_{st}(1 + s_b^2) - 2F_{bd}s_b}{F_{bd} - F_{st}} + s_b^2\right)s}{s^2 + \frac{F_{st}(1 + s_b^2) - 2F_{bd}s_b}{F_{bd} - F_{st}}s + s_b^2} \tag{88}$$

Where the starting torque F_{st}, the break-down torque F_{bd} and the corresponding slip s_b are given manufacturer data of the motor. Figure 12 illustrates the process of starting to open the bridge from closed position by a squirrel cage motor. The initial conditions of this system at t = 0 are the same as mentioned earlier in Equation 2. Then the equations of motion become

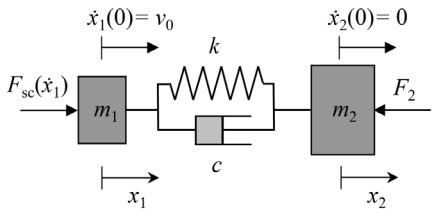

Figure 12. Opening from closed position with a force-speed characteristics of a squirrel cage motor

$$m_1\ddot{x}_1 + c(\dot{x}_1 - \dot{x}_2) + k(x_1 - x_2) = F_{sc}(\dot{x}_1) \tag{89}$$

$$m_2\ddot{x}_2 + c(\dot{x}_2 - \dot{x}_1) + k(x_2 - x_1) = -F_2 \tag{90}$$

6.2 *Modelling of a slip ring motor*

A slip ring induction motor, also called a wound-rotor motor, provides a higher starting torque compared to a squirrel cage motor. The poles of the rotor are connected to slip rings and each pole is wired in series with a resistor, which reduces the field strength of the stator during start-up. The motor speed-torque characteristics is adjusted by switching off the resistors one by one in order to maintain a higher torque at higher speed. The effect of varying rotor resistance on the torque-speed characteristics of a wound-rotor induction motor is shown in Figure 13 [6]. Torque control by slip rings can be found in old existing bridge machineries. Nowadays, mainly induction motors with variable frequency drives are used. An overall function of the torque-speed function can be approached by a combination of a zig-zag function at lower speed and a torque-speed characteristics of a squirrel cage motor $F_{sc}(s)$ at higher speed as calculated in Section 6.

$$F_{sr}(s) = \begin{cases} F_{bd} + (b_0 s - \text{floor}(b_0 s))\, d_0 + d_1 + b_1 & \text{if} \quad s_0 < s \le s_b \\ F_{sc}(s) & \text{if} \quad s_b < s \le s_{ns} \end{cases} \tag{91}$$

where F_{bd} and $F_{sc}(s)$ are defined in previous section. Constants b_0 And b_1 are given and determine the frequency and amplitude of the zigzag function, and where d_0 and d_1 are computed as follows

$$d_0 = -b_0 + 2b_0 \quad \text{mod}(\text{floor}(b_0 s), 2) \tag{92}$$

$$d_1 = -b_0 \quad \text{mod}(\text{floor}(b_0 s), 2) \tag{93}$$

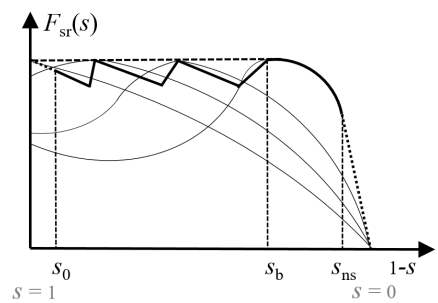

Figure 13. Force-slip characteristics of a slip ring motor $F_{sr}(s)$, approached by a zig-zag function

Figure 13 shows the process of starting to open the bridge from closed position by a slip-ring motor. The initial conditions at $t = 0$ are the same as mentioned earlier in Equation 2. Then the equations of motion become

$$m_1\ddot{x}_1 + c(\dot{x}_1 - \dot{x}_2) + k(x_1 - x_2) = F_{sr}(\dot{x}_1) \tag{94}$$

$$m_2\ddot{x}_2 + c(\dot{x}_2 - \dot{x}_1) + k(x_2 - x_1) = -F_2 \tag{95}$$

6.3 *Modelling of an emergency stop*

The concept of a rectangular pulse function can also be used in case of a speed-varying force such as the braking force $F_{br}(\dot{x})$, which acts in opposition to the motion of the motor shaft. If we consider the load situation *braking at full speed*, the braking force will be applied at nominal speed $\dot{x}_{ns}$ until the shaft stops rotating. The application of the braking force can be described by a rectangular pulse function as shown in Figure 15. Taking the discontinuities at $\dot{x} = 0$ and $\dot{x} = \dot{x}_{ns}$, we can use the Heaviside step function $H(\dot{x})$ in order to write the following equation for the velocity-dependent braking force $F_{br}(\dot{x})$

$$F_{br}(\dot{x}) = F_{br\max}(H(\dot{x}) - H(\dot{x} - \dot{x}_{ns})) \tag{96}$$

where $F_{br\max}$ is the maximum decelerating force of the brakes. However, the braking force is a sort of friction force. Therefore, we use a common friction smoothing procedure, which approximate the discontinuous friction at zero relative velocity and nominal speed by a smooth function as shown in Figure 16. Hence, before applying the braking force, the velocity of the system is at nominal speed. Then after applying the braking force on the first mass m_1, the velocity decreases until the system stops $\dot{x}_1 \le 0$. After that, the braking force $F_{br}(\dot{x}_1)$ will be the same as the reaction force in the powertrain. Substituting $\dot{x} = \dot{x}_1$ for the velocity of the motor shaft and rewriting Equation 96 we obtain

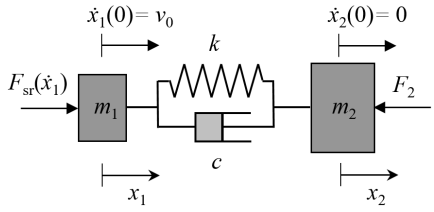

Figure 14. Opening from closed position with a force-speed characteristics of a slip-ring motor

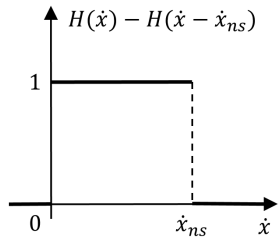

Figure 15. Rectangular pulse as a function of velocity

$$F_{br}(\dot{x}_1)=\begin{cases} F_{br\max}\left(\frac{2}{\pi}\arctan(c_1\dot{x}_1)-\frac{2}{\pi}\arctan(c_2\dot{x}_1-c_2\dot{x}_{ns})-1\right) & \text{if} \quad 0<\dot{x}_1\le\dot{x}_{ns} \\ c(\dot{x}_1-\dot{x}_2)+k(x_1-x_2) & \text{if} \quad \dot{x}_1\le 0 \end{cases} \tag{97}$$

where c_1 and c_2 are factors, which determines the rate of the smoothing approximation to the maximum, respectively, at zero and at rated velocities as shown in Figure 16. Multiplication by the quotient $\frac{\pi}{2}$ is to let the smoothing curve approach unity at its maximum value. However, the first two terms between parentheses of Equation 97 add up to 2, therefore, we subtract 1 from the sum. Then the equations of motion become

$$m_1\ddot{x}_1+c(\dot{x}_1-\dot{x}_2)+k(x_1-x_2)=-F_{br}(\dot{x}_1) \tag{98}$$

$$m_2\ddot{x}_2+c(\dot{x}_2-\dot{x}_1)+k(x_2-x_1)=-F_2 \tag{99}$$

7 Case study 1: Effect of different motor characteristics

In this section, the motor torque characteristics of a squirrel cage and a slip ring motor are investigated to demonstrate how they can influence the dynamic forces in bridge machineries. In order to investigate the effect of time-dependent excitations on dynamic behaviour of movable bridges during *opening from closed position*, predictions of an undamped model with constant loads, are compared with the results of a damped model with externally applied forces following specific torque-speed characteristics. The undamped model is shown in Section 2 as mentioned by Stroosma in [1]. The numerical values used for all models are presented in Table 3 and case specific quantities are provided in Table 4. The results are based on a numerical integration procedure using MATLAB.

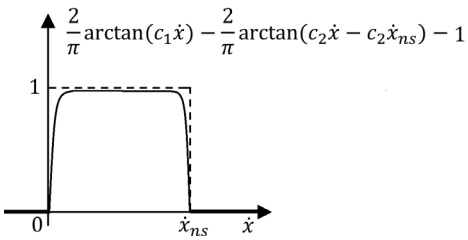

Figure 16. Smoothing of the braking force $F_{br}(\dot{x}_1)$ using an arctan-type approximation. Multi-valued braking force at zero and rated velocities are neglected.

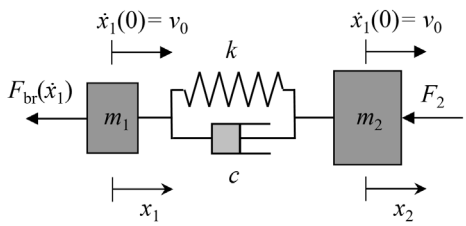

Figure 17. Braking the bridge with a nonlinear pulse function, while opening the bridge with constant speed

We compare the results of the occurring dynamic loads in the powertrain of the movable bridge of Table 3, while opening the bridge deck from closed position by both types of electric motors. The torque-speed characteristics are described in Section 6.

Table 3. Parameters of the semidefinite model for case study 1

Model data	Symbol	Value	Unit
Inertia of driver components	m_1	0.175	kgm²
Inertia of driven components	m_2	0.117	kgm²
Stiffness of driveline	k	2.50	Nm/rad
Damping constant of driveline	c	0.054	Nms/rad
Applied force by the driver	F_1	19.11	Nm
Static torque on driven side	F_2	7.35	Nm
Accelerating/decelerating force	F_a	11.76	Nm
Nominal speed while opening	$\dot{x}_{ns}$	102.1	rad/s
Starting speed	$\dot{x}_0 = v_0$	0	rad/s
Damping ratio	ζ	0.05	–

Moreover, we compare the prediction of the dynamic loads by an undamped and damped model with constant excitation, as mentioned respectively in Section 2 and 3. These predictions are also compared to the results, when calculated according to the rule, stated in the code NEN 6786:2017 for the load situation *opening from closed position*. The used speed-torque characteristics, of the squirrel cage motor (solid red curve), slip ring motor (dotted green curve) and a constant force (dashed blue curve), are shown in Figure 18 top. Figure 18 bottom shows the torque-speed characteristics of a slip ring motor for three cases. Note that the first case (dotted blue curve), when $b_1 = 0$, corresponds with a constant force between $s_0 \leq s < s_b$. For $b_1 = -3$ the green dotted curve shows the torque-speed characteristics of the slipring motor with a zigzag function. The bigger b_1 is, the higher this amplitude of the zigzag function becomes. For $b_1 = -6$ the amplitude increases as shown with the dotted cyan curve. In this section, we investigate the effect of this amplitude on the dynamic forces in the powertrain of the movable bridges. The numerical values of the used parameters are presented in Table 4.

The torque-speed characteristics in Figure 18 bottom leads to torque-time characteristics as

shown in Figure 19 top. Note that all curves have the same maximum value as expected. The differences are in the course of the curves. The slip-ring motor with $b_1 = -6$ (dotted cyan curve) shows more similarity with the torque-time characteristics of the squirrel cage motor (solid red curve) in the range of $s \leq s_b$.

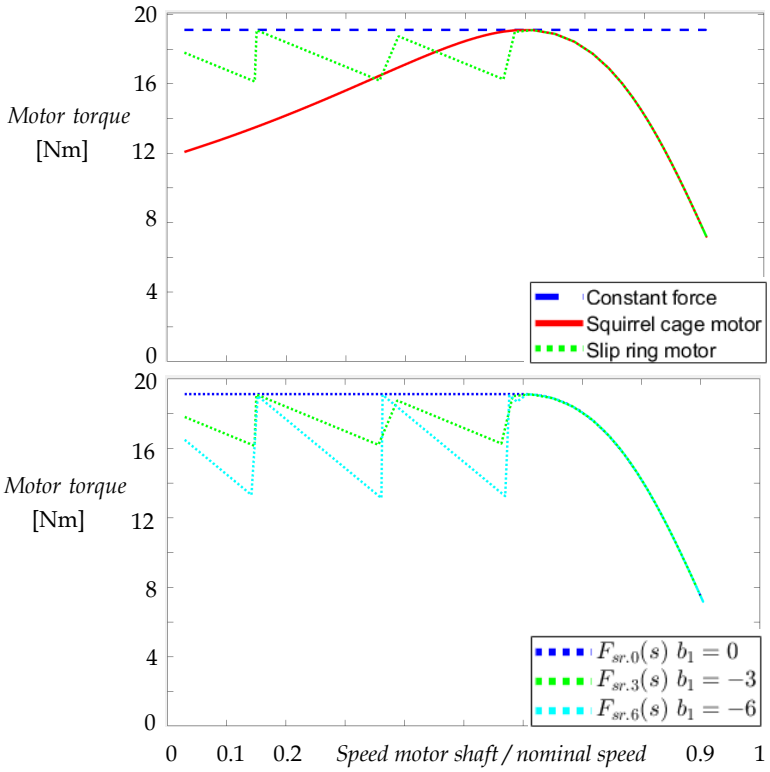

Figure 18. Motor characteristics. Top, torque-speed characteristics. Bottom, corresponding torque-speed characteristics of a slip ring motor with three different values of b_1 , which represents the amplitude of the zigzag function. If $b_1 = 0$, then the force is a constant.

Table 4. Parameters and model inputs of squirrel cage and slip ring motors

Squirrel cage motor	Symbol	Value	Slip ring motor	Symbol	Value
Breakdown slip	$1-s_b$	0.40	Frequency factor	b_0	4.7
Rated slip	$1-s_0$	0.03	Amplitude factor	b_1	0, -3, -6
Starting force	F_{st}	11.76 Nm	1st floor factor	d_0	Eq. 92
Breakdown force	F_{bd}	19.11 Nm	2nd floor factor	d_1	Eq. 93

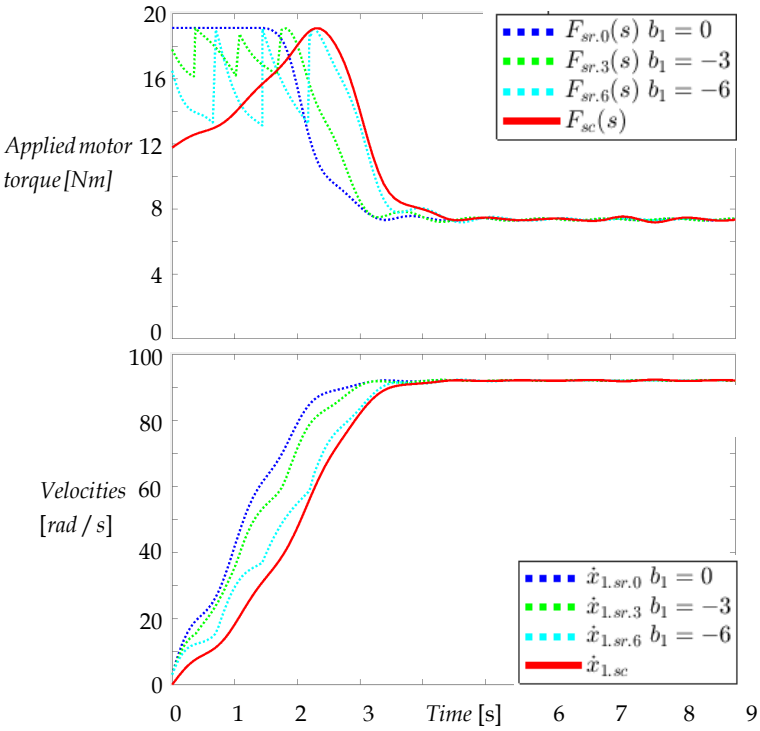

Figure 19. Top, torque-time characteristics of the squirrel cage and slip ring motors. Bottom, speed-time diagrams of the squirrel cage and slip ring motors

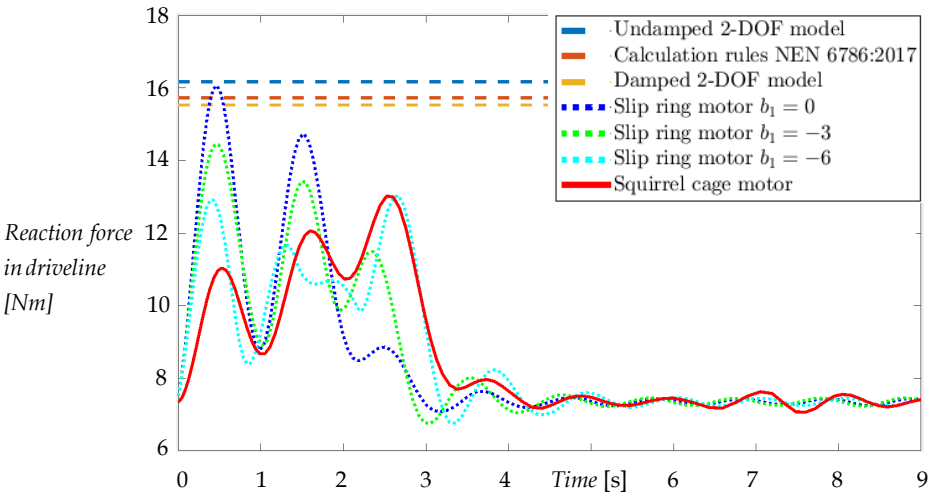

Figure 20. Occurring dynamic forces in the driveline, due to torques applied by the squirrel cage and slip ring motors, compared with the undamped and damped 2-DOF models and the calculation rules in NEN 6786 during opening from closed position

The torque-speed characteristics in Figure 18 bottom leads to torque-time characteristics as shown in Figure 19 top. Note that all curves have the same maximum value as expected. The differences are in the course of the curves. The slip-ring motor with $b_1 = -6$ (dotted cyan curve) shows more similarity with the torque-time characteristics of the squirrel cage motor (solid red curve) in the range of $s \leq s_b$.

Figure 20 shows the result of the obtained peak force according to different models. As expected, in case of applying the motor torque according to a speed-dependent motor characteristics instead of a constant force, the peak force in the powertrain becomes lower. As a result, we see a significant reduction in the dynamic peak forces obtained by the numerical models, compared to the analytical 2-DOF models and the calculation rules stated in the code. The amount of this reduction depends on the parameters.

For this case study, we obtain the following peak forces according to the different model types as shown in Table 5. Taking into account the motor characteristics will give a reduction of approximately 30% on the dynamic part of the total force *opening from closed position*.

Table 5. Peak forces according to the undamped and damped 2-DOF models with constant applied force F_1 , as well as the numerical solved models with speed-dependent characteristics $F_{sc}(\dot{x}_1)$ and $F_{sr}(\dot{x}_1)$

Model types	Value of peak forces
Undamped 2-DOF model	16.17 Nm
Calculation rules NEN 6786:2017	15.73 Nm
Damped 2-DOF model	15.53 Nm
Slip ring motor $b_1 = 0$	16.06 Nm
Slip ring motor $b_1 = -3$	14.45 Nm
Slip ring motor $b_1 = -6$	13.03 Nm
Squirrel cage motor	13.02 Nm

8 Case study 2: Effect of speed-dependent braking force

Finally, the load case *braking at full speed* is investigated. In order to explore the effect of a nonlinear braking force on the dynamic behaviour of movable bridges, predictions of a model with a constant maximum force are compared with the results of a speed-dependent braking force, which is following a specific arc-tangent smooth pulse function. The used dynamic model for this purpose is shown in Section 6, Figure 17. The numerical values used for the model are presented in Table 6 and case specific quantities are provided in Table 7. Figure 16 shows how the braking force $F_{br}(\dot{x})$ can be approached using an arctan-type approximation. By using different values for the smooth factors c_1 and c_2 as described in Equation 97 the plot of Figure 21 top can be drawn. Subsequently, these torque-speed characteristics leads to the torque-time characteristics as shown in Figure 21 bottom. Note that all the curves must have the same maximum value in order to ensure

Table 6. Parameters of the semidefinite model for case study 2

Model data	Symbol	Value	Unit
Inertia of driver components	m_1	0.175	kgm²
Inertia of driven components	m_2	0.117	kgm²
Stiffness of driveline	k	11.9	Nm/rad
Damping constant of driveline	c	0.118	Nms/rad
Applied force by the driver	$F_{br.\max}$	26.98	Nm
Static torque on driven side	F_2	-1.4	Nm
Accelerating/decelerating force	F_a	-25.58	Nm
Nominal speed while closing	$\dot{x}_{ns}$	-102.1	rad/s
Equilibrium speed after braking	$\dot{x}_0 = v_0$	0	rad/s
Damping ratio	ζ	0.05	–

Table 7. Various smooth factors of the braking pulse function

Pulse function	Symbol	Value
1st smoothing factor	c_1	0.05, 0.1, 1, 10
2nd smoothing factor	c_2	0.05, 0.1, 1, 10

the comparability of the different curves. Therefore, the smoothed functions have to be multiplied with a correction factor. Hence, the differences are only in the course of the curves depending on the speed. Similarly to the speed-time diagram of Figure 19 bottom, the more the braking force is smoothed, the less steep the course of the speed curve is. Subsequently, also in this case study the speed-time diagram is affecting the occurring dynamic forces in the powertrain, because, as mentioned before, the derivative of the speed is acceleration, which is directly related to the force. Figure 22 shows the result of the

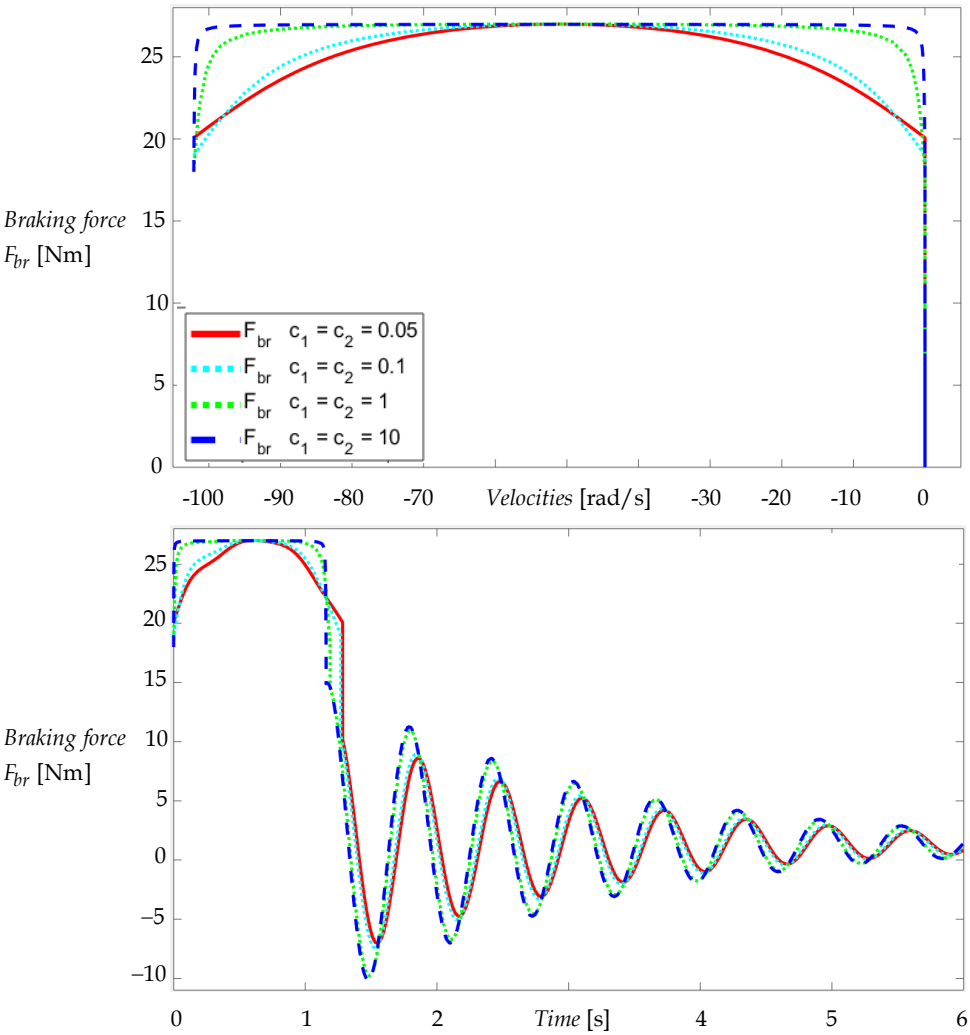

Figure 21. Braking force characteristics. Top, torque-speed characteristics. Bottom, corresponding torque-time characteristics at different values for the smoothing factor c_1 and c_2

Table 8. Peak forces according to the undamped and damped 2-DOF models with constant applied force F_1, as well as the numerical solved models with speed-dependent characteristics $F_{br}(\dot{x}_1)$

Model types	Value of peak forces
Calculation rules NEN 6786:2017	20.37 Nm
Arctan pulse with factors $c_1 = c_2 = 10$	19.97 Nm
Arctan pulse with factors $c_1 = c_2 = 1$	19.74 Nm
Arctan pulse with factors $c_1 = c_2 = 0.1$	18.10 Nm
Arctan pulse with factors $c_1 = c_2 = 0.05$	17.54 Nm

obtained peak force according to the models. As expected, in case of applying the smoothed braking torque, accordingly, the peak force in the powertrain becomes lower. As a result, we see a significant reduction in the dynamic peak forces obtained by the numerical models, compared to the calculation rules stated in the code NEN 6786:2017. The amount of this reduction depends on the smooth factors c_1 and c_2. For this case study, we obtain the following peak forces according to the different model types as shown in Table 8. Taking into account the smoothed braking characteristics will give a maximum reduction of approximately 14% on the dynamic part of the total force in the spring during *braking at full speed*.

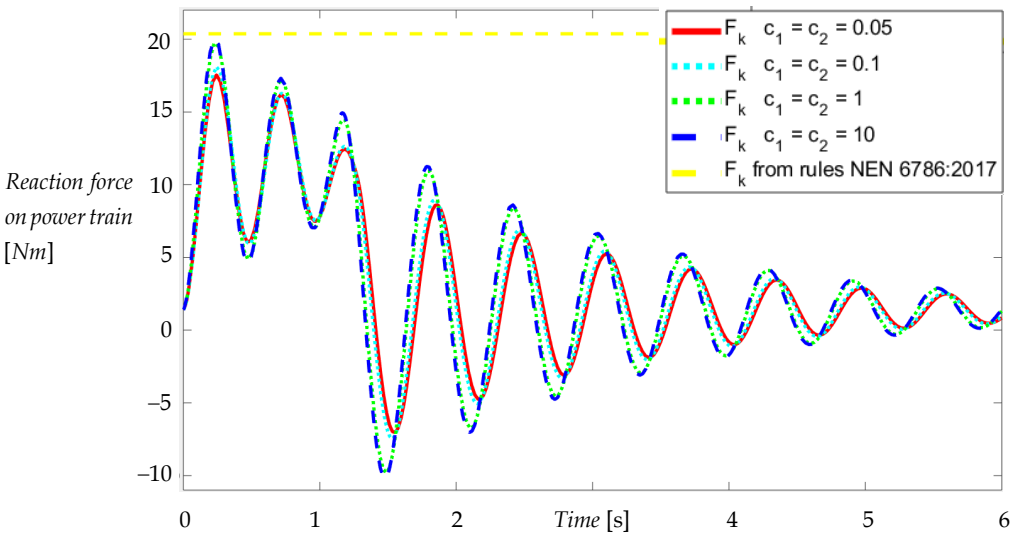

Figure 22. Occurring dynamic forces in the driveline, due to the applied braking torques, during load situation braking at full speed

9 Conclusions

In this paper, the effect of damping as well as time-varying excitations on the dynamic forces occurring in the powertrain of movable bridges are investigated and compared to the calculation rules stated in the Dutch design code for movable bridges NEN 6786 based on 2-DOF mass-spring-damper models.

First of all, three load situations, respectively, *opening from closed position*, *acceleration or deceleration* and *braking at full speed* are analysed with semidefinite 2-DOF models. A table is provided with slightly different calculation rules compared to the standard during mentioned load situations for calculating the decisive dynamic torques in the powertrain of movable bridges. Moreover, in contradiction with the calculation rules, it is shown that the effect of damping is not negligible for different bridge types, but depends on damping ratio ζ of the system. Especially in case of bascule bridges with push-pull rods or drawbridges, the dynamic amplification factor Φ_a, which is assumed to be equal to 1.9 for all movable bridges, is reduced significantly. A damping-dependent factor Φ_ζ is introduced that gives more realistic outcomes of the dynamic forces.

Secondly, the paper establishes a nonlinear numerical model for dynamic force predictions during *opening from closed position* due to the motor torque. The model consists of opening the bridge by torque regulated squirrel cage or slip ring motors using their torque-speed characteristics. A classical method is applied for calculating the torque speed curve of a squirrel cage motor. However, a novel analytical method is proposed to approach the torque characteristic of a slip ring motor in accordance with its manufacturing data. The first case study 26 was to compare the results obtained when using the proposed nonlinear models to the calculation rules derived from 2-DOF models of movable bridges with constant motor torques. The results show a significant reduction in the dynamic forces in the powertrain during *opening from closed position* compared to the theoretical predictions according to calculations in the standard.

Finally, the braking torque characteristic during the load situation *braking at full speed* is investigated. An analytical modelling approach is developed for the applied braking force by using a pulse function. The speed-dependency effects are considered in the analytical approach by using arc-tangent smooth factors. The braking torque characteristic is presented by an analytical formula in which the influence of the smooth factors on the

braking torque is demonstrated. Then the load situation *braking at full speed* is investigated by a study case with various torque characteristics in numerically solved models. It is shown that the results obtained from the models with noticeable smooth factors give a significant reduction of the dynamic peak forces in the powertrain compared to the analytical calculation rules based on constant braking forces.

Future work will focus on dynamic models for speed regulated machineries as well as modelling nonlinear variables as clearances and the stiffness of push-pull rods in bridge machineries. For the purpose of model verifications and validations, theoretical predictions will be compared to available data gathered from experimental research, lab and on-site measurements. Also attention will be given to a more realistic time dependent model for F_2 , which represents the gravity and wind forces on the bridge.

Acknowledgment

This publication is part of the PhD research on dynamics of movable bridges. The authors gratefully acknowledge the Dutch Ministry of Infrastructure and the Environment (*Rijkswaterstaat*), the Province of South-Holland and Antea Group Netherland for financing this project. Also the support for the realisation of an experimental test rig provided by the following sponsors are greatly appreciated: Prorail, Municipalities of Amsterdam and Rotterdam, Hollandia Services and Infra, SEW-Eurodrive, Flender, SKF, Boone B.V., DEMO, Kobout and FdGd.

References

[1] D. Stroosma, Dynamics of movable bridges, part I: drive machinery, Technical report, RWS directie bruggen (1980).

[2] NEN 6786:2001, Rules for the design of movable bridges, NEN (2001).

[3] NEN 6786:2017, Rules for the design of movable bridges, NEN (2017).

[4] P. Aree, Analytical approach to determine speed-torque curve of induction motor from manufacturer data, *Procedia Computer Science*, 86:293–296 (2016).

[5] P.W.P. van Staalduinen, Measurements of damping on six movable bridges, Technical Report B-90326, TNO (1990).

[6] J.F. Gieras and I. Gieras, *Electrical Energy Utilisation*, ISBN: 83-7174-199-5, 73-75 (1998).